FUDMA Journal of Sciences (FJS)
ISSN online: 2616-1370
ISSN print: 2645 - 2944
Vol. 6 No. 6, December, 2022, pp 22 - 30
DOI: https://doi.org/10.33003/fjs-2022-0606-1130

THE CORRELATION OF MICROSTRUCTURE, AND MECHANICAL PROPERTIES OF NOVEL Fe_3O_4-($AuTe_2$) –REINFORCED ALUMINIUM MATRIX COMPOSITE PRODUCED VIA RECRYSTALLIZATION ROUTE

***[1]Dankulu M. H., [2]Musa M., [3]Ibrahim M., [4]Sani S.**

[1]Department of Energy and Applied Chemistry, Usmanu Danfodiyo University Sokoto, Nigeria
[2]Sokoto Energy Research Centre, Usmanu Danfodiyo University Sokoto, Nigeria
[3]Department of Mechanical Engineering, Usmanu Danfodiyo University Sokoto, Nigeria
[4]Department of Pure and Environmental Chemistry, Usmanu Danfodiyo University Sokoto

*Corresponding authors' email: murtalahassandankulu@gmail.com

ABSTRACT

Aluminum Metal Matrix Composites (AMMC) have been becoming suitable materials for many devices in the application of various fields such as medical equipment, aircraft, electrical motors, overhead transmission lines, construction, etc. Aluminum was reinforced with the Fe_3O_4-($AuTe_2$) through the recrystallization process, hence, AMMC was successfully developed. The aim was to characterize the microstructure and phase patterns of the developed AMMC and compare it with conventional Aluminum as well as its thermos-mechanical characteristics. Physical, mechanical, and morphological properties of the composite and regular Al were examined. Based on the outcomes, the microstructural examination of the composite showed that the Al matrix had a sizable distribution of reinforcement components. Additionally shown was the creation of new phases, which significantly improved the strength and corrosion resistance of the composite. The influence of the reinforcement materials was found to have greatly enhanced the hardness tests. From 60 HRB for ordinary Al to 92.3 for AMMC, the hardness rose. Hence, after corrosion tests in an acidic solution (5% H_2SO_4 + H_2O) hardness also increased from 41.1 HRB of the conventional Al to 52.8 HRB of the AMMC. Therefore, Corrosion resistance is improved by adding this reinforcement (Al- Fe3O4-($AuTe_2$) to the composite (lower corrosion rate). We then chose Al-5Fe3O4-10($AuTe_2$) as an optimal composite after comparing all the samples.

Keywords: microstructure, solar still, corrosion behavior, hardness, recrystallization

INTRODUCTION

Currently, the primary materials being explored to address the technological, economic, and environmental challenges are metal matrix composites. Due to its superior strength, great wear resistance, and good dimensional stability, aluminum is one of the most widely used materials in the creation of metal matrix composites (Sakthivelu *et al.*, 2020). Composites made of aluminum are becoming more popular in the structural and automotive industries. Over traditional engineering materials like ferrous materials, these Al-MMCs have advantages, particularly in the decrease of weight that results in lower moment inertia, less fuel consumption, as well as superior corrosion and wears resistance (Roshan *et al.*, 2013). When viewed from a scientific and technological standpoint, the Al-MMCs are excellent candidates for a variety of applications due to their commendable mechanical qualities and fair cost-effectiveness in terms of production (Saravanan *et al.*, 2015). Aluminum metal matrix composites (AMMCs) are a viable alternative to conventional materials for a wide range of industrial applications due to their appealing properties, which include excellent corrosion resistance, a high strength-to-weight ratio, a low thermal expansion coefficient, good casting ability, lower density, higher strength, increased wear resistance, improved fatigue resistance, and improved stability at high temperatures. (Sharma *et al.*, 2018). Many investigations studies in the fields of engineering and materials science to produce composites and nano-composites with distinctive properties, which are typically attributed to the size of the reinforcing materials, their dispersion in the matrix, and the grain size of the matrix particles. Carefully combining additive particles results in a homogeneous dispersion into the matrix (Ferreira *et al.*, 2018). Fabrication methods for aluminum metal matrix composites include infiltration, powder metallurgy, squeeze casting, semi-solid casting, and stir casting (Kavimani *et al.*, 2019).

Magnetite (Fe_3O_4), is an iron ore magnet and one of the significant iron ores, which magnetic material is the most prevalent on earth (Ashrafi *et al.*, 2021). Because it is readily available, reasonably priced, and reacts with aluminum to produce a lot of free energy, magnetite is thought to be a suitable filler. By creating wettability between the aluminum and the magnetite in this reaction, more energy is provided for the remaining steps of the process. (Wang *et al.*, 2021).

The objective of this research is to characterize the microstructure and phase patterns of the developed AMMC as well as its thermos-mechanical characteristics. It is important to note that this research's findings will aid in the creation of a novel matrix composite in terms of discovering a composite which can be considered for application as an absorber for solar thermal materials.

Alaneme *et al.*, (2019) reported that metal matrix composites (MMCs) are created by combining two or more materials having different chemical, physical, and mechanical characteristics that are mechanically held together due to the variance in their coefficients of thermal expansion. The reinforcement is the hard, discrete material evenly distributed throughout the matrix, whereas the soft metal or alloy serves as a continuous portion and is known as the matrix. One of the key needs in the systemization of the MMCs is the significant difference between the melting temperatures of the matrix and reinforcement. As a result, the physical, chemical, and mechanical properties of MMCs are fundamentally different from those of the matrix and reinforcement that make up their composition. In prior work, Narayan and Rajeshkannan. (2011) found that the sintering techniques, such as temperature, lubrication regime, and compacting load.

Singh *et al.*, (2020) reported that the emission of CO_2 and other toxic residues, which is a significant contributor to pollution, must be reduced by designers, scientists, and engineers. The biggest issue is the vehicle's weight. Both the

decrease in emissions and the improvement of the vehicle's efficiency are directly impacted by its lowering. Rapid-flow mixing and high-pressure compositing were used to strengthen a high chromium cast iron matrix with zirconia-toughened alumina. Qiu *et al.* (2019) distinct and robust interface between them was created by the uniform distribution of reinforcement across the matrix. The matrix was less resistant to wear than the composite. According to reports, as impact energies increased, the wear mechanisms changed.

A stud by Alfattani *et al.,* (2022) Al alloys are more expensive than steel, have a lower modulus than steel, and necessitate special welding techniques because of their abrasive nature. Even when exposed to air, a thin layer of Al oxide on the metal's surface prevents oxidation. Depending on the method to be utilized in the weld joints (such as heat or pressure), pressure and non-pressure welding are used to combine comparable or dissimilar materials. Pressure welding (such as diffusion and friction stir welding) uses external pressure to compel two components to merge at temperatures below melting without the need of a filler material and without altering the properties of the original material because the base metals do not melt. In engineering activities, aluminum matrix composites (AMCs) are receiving more attention (Manikandan and Arjunan, 2020).

Prior studies have focused on the fabrication of hybrid aluminum matrix composites with two or more reinforcements, such as SiC particles with carbon nanotubes (CNT) or Al_2O_3 reinforced aluminum matrix composites (AMC) mechanical properties (Prakash *et al.,* 2020). However, the roll-bonding method of producing the aluminum-based composite was examined, and the mechanical characteristics of the aluminum matrix composite reinforced with E-type glass fiber were researched. They came to the conclusion that the resulting composites' strength greatly increases along with an increase in rolling cycles, which is accompanied by a concurrent decrease in elongation as compared to the base material (aluminum EN AW 1050) (Alizadeh *et al.,* 2019). Al_2O_3, ZrO_2, and TiC, as well as Fe_2O_3, Fe_3O_4, Ag, and Co, are just a few of the added materials utilized today to enhance mechanical, electrical, or magnetic capabilities. The efficiency of solar cells can also be increased by using additional additives, such as semiconductor photo anode materials Fe_2O_3, ZnO, TiO_2, W, O_3, and $BiVO_4$ (Liu et al., 2021). Fe_2O_3 and Fe_3O_4 have drawn a lot of attention because of their special qualities, including being simple to make, inexpensive, non-toxic, and thermodynamically stable. Fe_2O_3 has a variety of crystal phases that make it useful for many different things, including biological and medicinal uses, adsorbents, and photocatalysts (Jian et al., 2019).

Samal *et al.,* (2020) while a literature review revealed that MMC researchers frequently discuss their materials' superior strength-to-weight ratio, one of their most alluring qualities. However, there was not a single paper that examined the strength-to-weight of MMCs in great detail. In order to compare established AMMCs with emerging MMCs objectively, particular aspects of each must be considered. When taken into account simultaneously in a holistic manner, physical characteristics like density and porosity, in addition to mechanical characteristics, have a significant influence.

Investigations on aluminum Composite matrix with an emphasis on magnetic features showed that Fe_3O_4 nanoparticles results in due to a boost in soft magnetic characteristics (Ashrafi *et al.,* 2020). Fathy *et al.,* (2015) studied on how the iron impacted on the mechanical, microstructure, and magnetic properties of AMCs. Maleki *et al.,* (2018) examined the magnetic nickel ferrite addition to aluminum. An aluminum matrix reinforced with nickel ferrite should result in a lightweight material with remarkable magnetic properties for use in a variety of applications, such as sensitive measurement tools, automobiles, and aircraft. As such, this study synthesized AMCs reinforced with $NiFe_2O_4$ nanoparticles to determine their magnetic characteristics, microstructure, and mechanical properties. Borghain *et al.,* (2012) produced magnetic composites with aluminum-scattered cobalt ferrite magnetic nanoparticles. With a Ms of 17.07 emu/g for the aluminum sample supplemented with 10 wt% cobalt ferrite, cobalt ferrite significantly advanced the magnetization estimation of the aluminum matrix. The Ms and Hc of the composite with 1 wt.% cobalt ferrite were found to be 3.51 emu/g and 967 Oe, respectively. However, with an increase in the ferrite content (10 wt.% cobalt ferrite) in the Al matrix, the Ms and Hc increased to 17.07 emu/g and 583, respectively. Strong physical characteristics of AMMCs (electrical and magnetic properties) allow them to be as lightweight as a multipurpose alloy. (Ferreira *et al.,* 2017). Additionally, the manufacturing process utilized to create nano-composites has an impact on the mechanical characteristics of AMNCs. To create composite and nano-composite materials, a variety of processing methods, including melting casting, and powder metallurgy, have been used. (Mummoorthi *et al.,* 2019).

From the literature reviewed, it is evident that previous research was focused on the materials for AMC and other related applications of composites and therefore, the application of composites technologies for solar thermal, and the recrystallization as a technique in composites fabrication with the use of ($AuTe_2$) and Fe_3O_4 as reinforcements in the aluminum matrix has not been reported in the literature to the best of the researcher knowledge. This study, therefore, focuses on the selection, development, and evaluation of composites materials that can resist higher temperature oxidation, stress, and fatigue and with optimum light trapping morphology to avoid structural and operational failures resulting from poor thermal, chemical, and mechanical properties of alloys and coatings currently being used in solar thermal materials.

MATERIALS AND METHODS

Recrystallization Technique

Commercially available aluminum (fine) powder with a purity of 99.7% was purchased from (MolyChem Industrial Co., Ltd., India) and an average particle size of 200 mesh (74 µm) was used as the composite matrix. *Magnetite (Fe_3O_4) and silver-gold telluride ($AuTe_2$)* were used to reinforce the Al matrix. The materials were crushed, ground, and sieved to obtain small particle sizes. All samples of composites were diligently carried out by the recrystallization process, and the mixture of the powders of aluminum (as metal matrix), Fe_3O_4, and ($AuTe_2$) (the reinforcements) at different weight percentages, the samples were mechanically milled for 30 minutes using a Ball mill (Bm500, Antopaar, Austria), at 20 Hz at room temperature to ensure that additional components are distributed evenly and dispersed into Aluminium matrix. The sample was placed inside the furnace for heating at 600ºC for 1hr. The samples were allowed to cool in the furnace chamber, then heating was continued for 1 hour at 780ºC. Later, the sample was removed from the furnace. The sample compositions of the AMCs are presented in Table 1. A small amount of each of the samples was prepared samples by polishing with file and taken for analysis purposes of the microstructural characterization.

Table 1: Different compositions of aluminum, magnetite and gold-silver telluride

S/N	SAMPLE	COMPOSITIONS (wt %)		
1	**A**	**Al 75**	**(Au,Ag)Te_2 15**	**Fe_3O_4 10**
	B	Al 65	**(Au, Ag)Te_2 20**	**Fe_3O_4 15**
3	C	Al 55	**(Au, Ag)Te_2 25**	**Fe_3O_4 20**
4	D	Al 45	**(Au, Ag)Te_2 30**	**Fe_3O_4 25**
5	E	Al35	**(Au, Ag)Te_2 35**	**Fe_3O_4 30**

Characterization

Phase and Microstructural Analysis

XRD analysis. X-ray diffractometer, (Rigaky mini flex model: XRD 300/600 Texas, USA) was used to record the XRD pattern of Aluminum reinforced with Fe_3O_4 and ($AuTe_2$) for phase analysis with a scan range from 3 – 90 operating at 40 kV and 15 mA, with a scanning speed of 10º 2-theta (2θ) and step size of 0.01º. Scanning electron microscopy (SEM). Scanning electron microscopy (Phenom prox SEM, generation 5, Switzerland), using a 2 kV acceleration voltage, the particle morphologies and microstructure were revealed. The microstructural investigation focused on the surface of sample. The samples were then subjected to Scanning electron microscopy to examine their microstructures. Energy Dispersive Spectroscopy (EDS) was carried out on the surfaces of the samples to uncover the phases present in the composite.

Hardness test

Hardness test is frequently employed for material evaluation since it is straightforward and inexpensive compared to direct measurement of many attributes. With this technique, the test material is indented using a diamond cone or a hardened steel ball indenter. Under a preliminary light load F0 typically, the indenter was pressed into the test material 10kg. An indicating device that tracked the indenter's movements and hence responded to variations in the depth of penetration of the indenter was set to a datum location after equilibrium had been established. A second big load was applied, increasing penetration while the initial small load was still in place. The additional major load was removed but the initial minor load was kept in place till equilibrium had been restored. By removing the extra significant weight, the depth of penetration can be decreased partially. The application and removal of the additional main load resulted in a permanent increase in penetration depth, which was utilized to determine the Rockwell hardness number. In the present experimental work, Rockwell hardness was measured on the sintered and recrystallized Al-Matrix Composites samples. For each of the samples, the test was conducted three (3) times and the average was taken as the result.

Figure 1: Rockwell hardness tester

RESULTS AND DISCUSSIONS

Microstructure Examination Results

The results obtained from Scanning Electron Microscope (SEM) for the samples Al-10Fe_3O_4-15($AuTe_2$) and Al-30Fe_3O_4-35($AuTe_2$) are shown in figure 3.1a,b, revealed that the materials has a rectangular shape with particle size that range from 10mm to 16mm with an average of 12mm. Figure 4.1a & b shows growth of grain size and fairly uniform distribution of Fe_3O_4 and ($AuTe_2$) particles in the aluminium matrix. ($AuTe_2$) appeared as a dark grey- Fe_3O_4 particles are the black-colored element, and they are spread relatively uniformly in the both sample. According to previous study by Ramakrishnan and Dinda, (2020) stated that the particle size distribution ought to be narrow as possible to ensure homogeneous energy, absorption in the matrix, which is influenced by a number of variables, including the pace of solidification and the quantity of reinforcement.

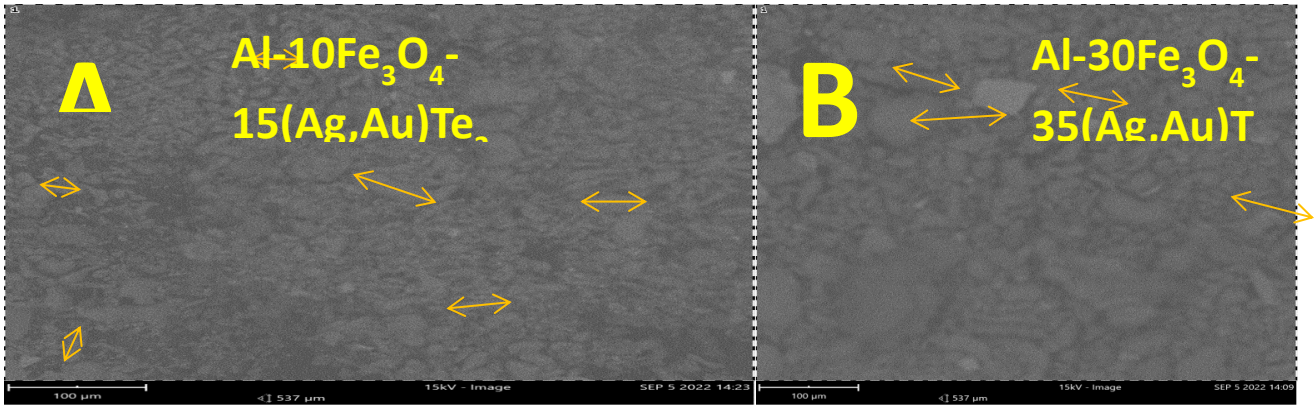

Figure 2: SEM image of (a) Al-10Fe_3O_4-15($AuTe_2$), and (b) Al-30Fe_3O_4-35($AuTe_2$).

Another similar result reported by Ashrafi *et al.*, (2020), The best reinforcement requires the solid attachment between the matrix and the particles. The result is in agreement with the finding of (Jawalkar *et al*., 2017 and Subri *et al.*, 2020) chemical bonding, inter-diffusion, and van der Waals bonding are the contents of interface mechanisms, matrix bonding, and reaction between the reinforcements and matrix in the composite, according to the findings of the current study. The mechanical and thermal properties of the composite could be negatively impacted by an excessive reaction between the particles and matrix, while a severe reaction could harm the reinforcements. (Jawalkar *et al*., 2017).

A previous study by Negin *et al.*, (2020) reported that For the manufacturing of composites, the optimum response is sought. Thermite reactions that self-sustain frequently contain magnetite. Thereby, Al–Fe_3O_4 system is identified as a highly exothermic reaction that can be employed during mechanical or thermal treatments, based on the following stoichiometric reaction:

$3Fe_3O_4 + 8Al \rightarrow 4Al_2O_3 + 9Fe \quad \Delta H^o = -3021\ kJ \quad (1)$

A study conducted by Sijo and Jayadevan, (2016) reported that one of the weak interface resultants the reduction in stiffness, hardness and strength, a high resistant to fracture. In contrast, a strong interface between particles in the matrix shows high stiffness and strength, but typically low resistance to fracture (Sulaiman *et al.*, 2017).

Similar results were reported in a study by Ravikumar *et al.*, (2017) the amount of reinforcement materials used and the hybrid composite's microstructure determine its mechanical properties. Al-Fe_3O_4 composites' microstructure was changed by the addition of gold-silver telluride, improving their mechanical properties. The telluride addition of gold and silver prevents recrystallization. With an increase in the gold-silver telluride content, the recrystallization has been more severely impeded. However, the recrystallization region's grain size has grown larger. (Wu *et al.*, 2014). Additionally, the production of numerous component particles is encouraged by silver. These constituents deplete the remaining hardening elements in the matrix by consuming hardening elements like Zn, Mg, and Cu, which damages the mechanical characteristics. (Wu *et al.*, 2014).

For the Al-Fe-($AuTe_2$) composition, at a temperature above 600ºC, Al_2Fe_3($AuTe_2$) is at a stable phase (Raghavan *et al.*, 2009). Figure 4.2 shows SEM image elemental composition of Fe_3O_4-(($AuTe_2$) reinforced Aluminium Matrix Composite with uniform distribution Fe_3O_4, and ($AuTe_2$) powders.

As reported somewhere else, by AzimiRoeen *et al.*, (2019) reported that Since the sintering process took place above 600ºC, the Al-Fe_3O_4 would undergo the following reactions: reduction of Fe_3O_4 through an intermediate reaction to form FeO, followed by reduction to Fe. The reaction can be written as;

$Fe_3O_4 \rightarrow 3FeO + 1/2O_2 \quad (2)$

$2Al + 3FeO \rightarrow Al_2O_3 + 3Fe \quad (3)$

$3Al + Fe \rightarrow Al_3Fe \quad (4)$

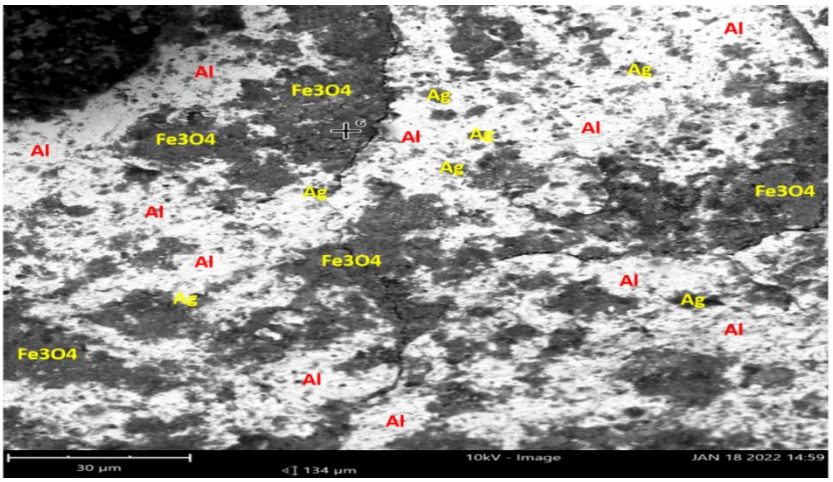

Figure 3: SEM image elemental compositions of Fe_3O_4-($AuTe_2$) reinforced Aluminium Matrix Composite.

The elemental compositions of Al-Fe_3O_4-($AuTe_2$) surface sample are shown in Figure 3 and were based on Figure 4. The exposed surface's EDS investigation yields an aluminum content of 83.50 wt%. In Fe_3O_4 particle (Dark color) exists in the aluminum matrix, with confirmed peaks of Fe (5.30 wt%), O (21.93 wt%) and Ag (0.22 wt%) respectively. Based on the EDS analysis, it indicates that the intermetallic phase of Al_3Fe and interfaces of Al_2O_5 occurred at some points in figure 4.3 with Al 89.16 wt%, Fe 8.07 wt%, and Al 83.50 wt% detected, respectively, which were also confirmed in to be in accordance with the XRD analysis.

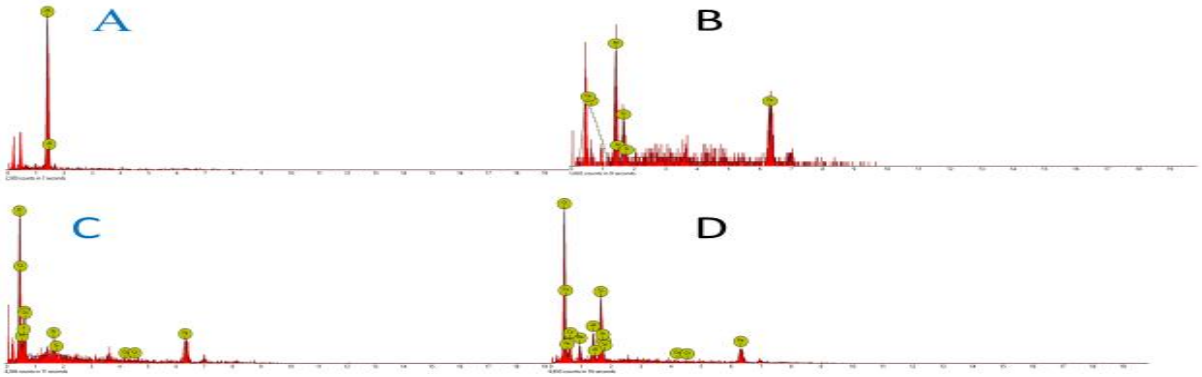

Figure 4: The EDS spectrum of Al-5Fe_3O_4-10($AuTe_2$) (a) Aluminum, (b) $AlFe_3$, (c)Fe_3O_4, (d) Al_2O_5 and (e) AgAl.

The SEM image for Al-30Fe_3O_4-35($AuTe_2$) is also shown in Figure 3.4 composites after sintering at above 600ºC. The Al matrix with a homogeneous distribution of Fe_3O_4 powders (black) and ($AuTe_2$) particles (dark-grey) was situated at the grain borders and was rectangular in shape. The matrix's homogeneous particle distribution is therefore obvious. The likelihood of agglomeration at grain borders also increases as the weight % of reinforcements increases. Additionally, the role of ($AuTe_2$) ore is to create new phases with the Al matrix and then to be diffused at the grain boundaries between Al grains and reinforcement. Moreover, the dispersion of ($AuTe_2$) is to reduce porosity before enhancing the mechanical characteristics (Salman *et al.*, 2022).

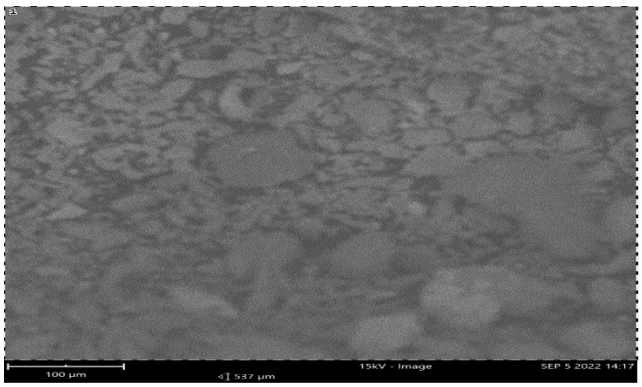

Figure 5: SEM image elemental compositions of Al-20Fe_3O_4-25($AuTe_2$) reinforced Aluminium Matrix Composite.

The SEM image elemental composition results from four areas of Al-30Fe_3O_4-35($AuTe_2$) sample surfaces, which are shown in Figure 5, and are presented in Figure 4.5. The elemental results show Al, Fe, Ag, Au, and O, in the grain boundaries. figure 3.4a there is aluminum, where Al peaks (87.18 wt%) are the main peak, and it is detected by using SEM, in white color, also in figure 4.4d Fe_3O_4 (Fe 6.02 and O 16.77 wt%) in black particles, and figure 3.4a another spot is confirmed as (Au, Ag)Te_2 (Au 11.42 and Ag 0.22 wt%) in a dark grey color, and they were also confirmed by XRD pattern. According to the EDS analyses, the compositions of Ag_3Al (Al 87.18 and Ag4.25 wt%), Al_2O_5 (Al 25.79 and O 16.77 wt%), and $AgAl_2Fe_3$ (Ag0.26, Al2.52 and Fe 1.62 wt%) at figure 3.5a,b, c, and d were detected, respectively, which were also confirmed by XRD pattern. This analysis is also in agreement with previous research (Negin *et al.*, 2020).

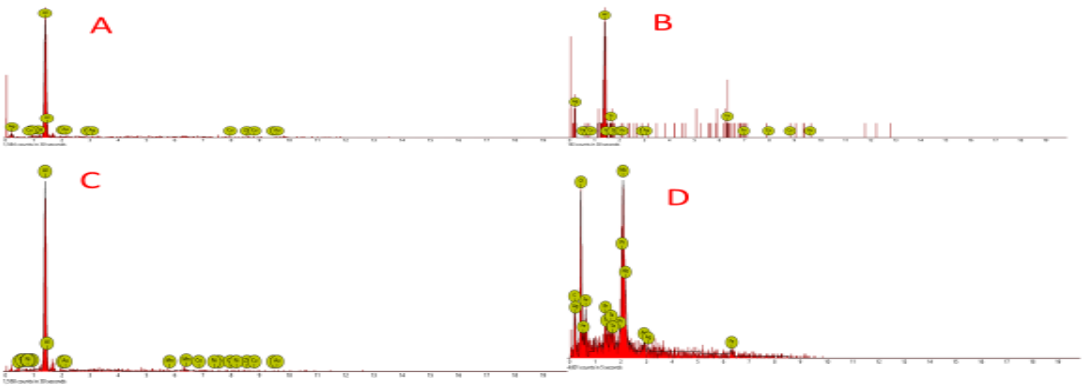

Figure 6: The EDS spectrum of Al-30Fe_3O_4-35($AuTe_2$) composition: (a) aluminum, (b) Fe_3O_4, (c) (Au,Ag)Te_2, (d) Ag_3Al, (e) Al_2O_5, (f) $AgAl_2Fe_3$, and (g) $AlFe_3O_4$-($AuTe_2$).

Results of X-ray Diffraction

The XRD analysis was carry out both before and after sintering. The XRD images of pure aluminium, Fe_3O_4 and (Au, Ag)Te_2 particles are shown in Figure 7 The XRD demonstrated five key peaks for aluminium (111, 200, 220,311, 222) as indicated with three main peaks for Fe_3O_4 as shown in Figure 4.6. Figure 4.6 also revealed the XRD analysis of samples J1 and J2 before and after heat treatment. The aluminium matrix has a face-centered cubic structure (FCC). After the addition of Fe_3O_4 and ($AuTe_2$) particles into aluminum, two peaks appeared, which refer to iron oxide and silver (Ag_2Te) with two crystal systems, Orthorhombic and Cubic, before heat treatment. Moreover, after heat treatment, two peaks disappeared which were assigned to Fe_3O_4 and silver. The XRD results after heat treatment identified Al-Fe intermetallic compounds Al_3Fe and Al_2O_3. Similar behavior was reported by Kumar *et al.*, (2009) in their study on Al 7075–Al_2O_3 MMCs, where the authors concluded that the hardness of the composites was enhanced with increased filler content.

The first peak is related to Fe_3O_4 with a cubic crystallography system. After adding Fe_3O_4 and ($AuTe_2$) particles into aluminium, and heat treatment, four main peaks were revealed for aluminium, one main peak for Fe_3O_4. 2θ = (38.4º, 44.70º, 65.0º, 70.1º, 78.0º) were associated with aluminium, and 2θ = (32.9º, 35.3º, 63.6º) was assigned to the Fe_3O_4 cubic crystal system. Thus, this shows that the intensity of the aluminium has decreased due to the loading of reinforcement and heating effects.

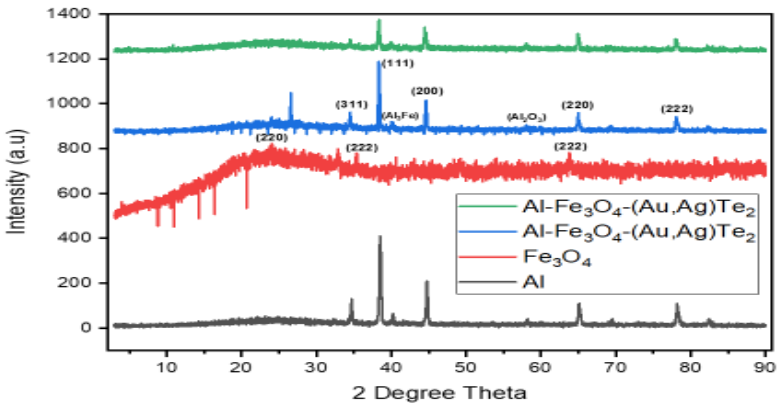

Figure 7: XRD analysis for (a) Aluminum, (b) Magnetite, (c) Gold-silver Telluride before sintering and after sintering.

Results of Mechanical Test

Micro-Hardness Test Result

Table 2: Rockwell hardness value of AMMC and conventional Aluminium

Specimen	Major Load (kgf)	Preliminary Load (N)	Penetrator	Scale	Reading	Rockwell hardness Value
Conventional Al after corrosion in (H_2SO_4)	100	9.81	1/16” Ball point	B	36.5 41 46	41.1
AMMC before corrosion	100	9.81	1/16” Ball point	B	91 93 93	92.3
	100	9.81	1/16” Ball point	B	35	52.8

AMMC after corrosion in (H_2SO_4)					58	
					48.5	
	100	9.81	1/16" Ball point	B	61	61
Conventional Al after corrosion in (NaCl)					65	
					56	
	100	9.81	1/16" Ball point	B	36	50
AMMC after corrosion in (NaCl)					46	
					68	

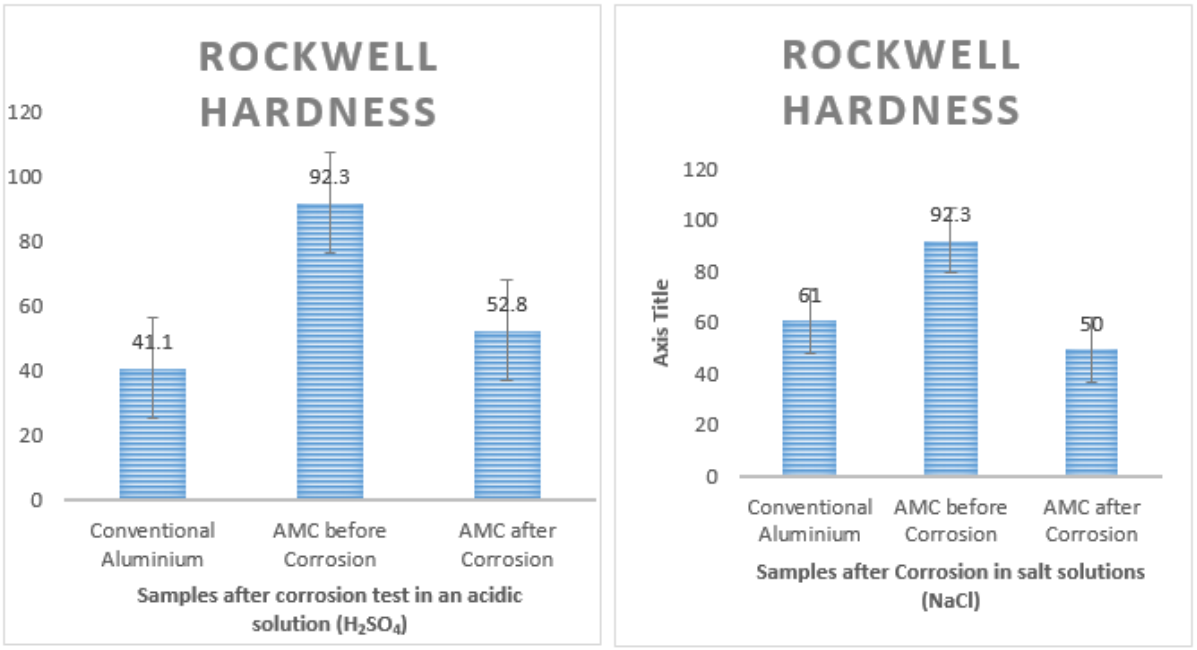

Figure 8: The variation of Rockwell hardness of conventional Aluminum, AMMC before corrosion and AMMC after corrosion.

The hardness value sustained by the samples before and after completing the corrosion test in the sulphuric acid solution for 6 hours and 8 hours for samples in salts solution is presented in figure 4.10. The conventional Aluminium in salt solution (NaCl) had a higher hardness value than the conventional Al in an acidic solution after the corrosion test. Hence, AMMC in an acidic solution shows higher hardness after corrosion than the AMMC in salts solution.

The hardness tests value were found to have improved significantly due to the impact of the reinforcement materials. The hardness increased from 60 HRB of the conventional Al to 92.3 of the AMMC. Hence, after corrosion tests in an acidic solution (5% H_2SO_4 + H_2O) hardness also increased from 41.1 HRB of the conventional Al to 52.8 HRB of the AMMC.

Therefore, the values for AMMC before and after the corrosion test in the sodium chloride solution can be observed to be 92HRB and 50HRB respectively. AMMC hardness were improved after the reinforcement. The study by Salman *et al.*, (2022) reported that the increase in the weight fraction wt.% of Fe_2O_3 and the steady wt.% of Ag leads to decreases in the porosity of nano-composites by filling the pores and then virtually affecting micro-hardness. Sasaki *et al.*, (2007) reported that the addition of 5 wt.% Fe in an Al matrix could lead to improvement in the mechanical properties of the alloys owing to grain refinement and the formation of intermetallic compounds such as Al_3Fe and Al_6Fe. Sijo and Jayadevan, (2016) reported that one of the weak interface resultants is the reduction in stiffness, hardness and strength, but highly resistance to fracture. A previous study by, Basariya and Mukhopadhyay, (2018) stated that this phenomenon occurred due to the influence of grain-size refinement, where crystallite size is decreased after the addition of Fe in Al. Finally, The hardness of the AMMC has shown considerable improvements on increased content of Fe_3O_4-(Au, Ag)Te_2 up to 5 wt. % to the Al matrix. Hence, the micro-hardness test is considered an important aspect to define the microstructures and mechanical properties of the materials (Chen *et al.*, 2011).

CONCLUSION

In this study, a nano composite (Al-Fe_3O_4-(Au, Ag)Te_2) was composed of an aluminium matrix reinforced by different wt.% of (Al-Fe_3O_4-(Au, Ag)Te_2). These reinforcement particles were successfully synthesized by recrystallization process. Various examinations have been performed for the samples of this work, such as Field Emission Scanning Electron Microscopy (FESEM) and X-ray Diffraction (XRD) analysis to estimate the microstructure and phases of manufactured composites. However, micro-hardness testing was assessed. Based on the obtained results it revealed that in addition of reinforcement particles into aluminum, the five composites show similar results for Al-Fe_3O_4 and (Au, Ag)Te_2 before and after sintering. The results of SEM and XRD demonstrate that Fe_3O_4 and (Au, Ag)Te_2 particles are uniformly distributed and dispersed into the Al matrix. The hardness tests were found to have improved significantly due to the impact of the reinforcement materials. The hardness increased from 60 HRB of the conventional Al to 92.3 of the AMMC. Hence, after corrosion tests in an acidic solution (5% H_2SO_4 + H_2O) hardness also increased from 41.1 HRB of the conventional Al to 52.8 HRB of the AMMC. The addition of this reinforcement in the AMCs shows a positive outcome toward corrosion resistance, in order to improve the durability

of material during operation. The accomplished results revealed that, not increasing the weight percentage of Fe_3O_4-($AuTe_2$), had improved the mechanical properties. After comparing all samples, we then selected Al-10Fe_3O_4-15($AuTe_2$) as an optimized composite. It is, therefore, recommended that the composite can be used for solar thermal-related applications.

REFERENCES

Alaneme, K. K, Okotete, E. A, Fajemisin, A. V, and Bodunrin, M. O. (2019). Applicability of metallic reinforcements for mechanical performance enhancement in metal matrix composites: a review *Arab Journal of Basic and Applied Sciences* **26** 311–30

Alfattani, R.; Yunus, M.; Mohamed, A.F.; Alamro, T.; & Hassan, M.K. (2022). Assessment of the Corrosion Behavior of Friction-Stir-Welded Dissimilar Aluminum Alloys. Materials.15, 260.

Alizadeh, M.; Shakery, A.; & Salahinejad, E. (2019). Aluminum-matrix composites reinforced with E-glass fibers by cross accumulative roll bonding proces. J. Alloys Compd. 804: 450-456.

Ashrafi, N., A.H. Mohamed Ariff, M. Sarraf, S. Sulaiman, & T.S. Hong. (2020). Microstructural, Thermal, Electrical, and Magnetic Properties of Optimized Fe_3O_4-SiC Hybrid Nano Filler Reinforced Aluminium Matrix Composite, *Materials Chemistry and Physics*, https://doi.org/10.1016/j.matchemphys.123895.

Ashrafi, N.; Ariff, A.H.M.; Sarraf, M.; Sulaiman, S.; & Hong, T. (2021). Microstructural, thermal, electrical, and magnetic properties of optimized Fe3O4–SiC hybrid nano filler reinforced aluminium matrix composite. Mater. Chem. Phys. 258: 123895.

AzimiRoeen, G.; Kashani-Bozorg, S. F.; Nosko, M.; & Lotfian, S. (2019). Mechanical and Microstructural Characterization of Hybrid Aluminum Nanocomposites Synthesized from an Al–Fe3O4 System by Friction Stir Processing. Met. Mater. Int. 26, 1441–1453.

Basariya, M.I.R.; & Mukhopadhyay, N.K. (2018). Chapter 5, Structural and mechanical behaviour `of Al-Fe intermetallics. In Intermetallics Compounds; IntechOpen: London, UK.

Borgohain, C.; Acharyya, K.; Sarma, S.; Senapati, K.K.; Sarma, K.C.; and Phukan, P. (2012). A new aluminum-based metal matrix composite reinforced with cobalt ferrite magnetic nanoparticle. J. Mater. Sci. 48: 162–171.

Fathy, A.; El-Kady, O.; & Mohammed, M. M. (2015). Effect of iron addition on microstructure, mechanical and magnetic properties of Al-matrix composite produced by powder metallurgy route. Trans. Nonferrous Met. Soc. China. 25: 46–53.

Ferreira, L. M.; Bayraktar, E.; Miskioglu, I.; & Robert, M. H. (2018). New magnetic aluminum matrix composites (Al-Zn-Si) reinforced with nano magnetic Fe_3O_4 for aeronautical applications. Adv. Mater. Process. 4: 358–369.

Ferreira, L.F.P.; Bayraktar, E.; Miskioglu, I.; & Robert, M. H. (2017). Recycle of aluminium (A356) for processing of new composites reinforced with magnetic Nano iron oxide and molybdenum. In Mechanics of Composite and Multi-functional Materials; Springer: Cham, Switzerland. 7: 153–161.

Jawalkar, C., A. S. Verma, & N. Suri. (2017). Fabrication of aluminium metal matrix composites with particulate reinforcement: a review, Materials. 4: 2927-2936.

Jian, W.; Wang, S.P.; Zhang, H.X.; & Bai, F.Q. (2019). Disentangling the role of oxygen vacancies on the surface of Fe_3O_4 and -Fe_2O_3. Inorganic Chem. Front. 6: 2660–2666.

Kavimani, V.; Prakash, K. S.; and Thankachan, T. (2019). Experimental investigations on wear and friction behavior of SiC@ r-GO reinforced Mg matrix composites produced through solvent-based powder metallurgy Compos. Part B Eng. 162: 508–521.

Kumar, P. R. S.; Kumaran, S.; Rao, T.S.; and Siva Prasad, K. (2009). Microstructure and mechanical properties of fly ash particles reinforced AA6061 composites produced by press and extrusion. Trans. Indian Inst. Met. 62, 559–566.

Liu, Y.; Zhao, G. J.; Zhang, J. X.; Bai, F.Q.; & Zhang, H. X. (2021). First-principles investigation on the interfacial interaction and electronic structure of $BiVO_4/WO_3$ heterostructure semiconductor material. Appl. Surf. Sci. 549, 149309.

Machaka, R. & Chikwanda, H. K. (2015). Analysis of the Cold Compaction Behavior of Titanium Powders: A Comprehensive Inter-model Comparison Study of Compaction Equations *Metallurgical and Materials Transactions A* **46** 4286–97.

Maleki, A.; Taherizadeh, A.; Issa, H.; Niroumand, B.; Allafchian, A.; & Ghaei, A. (2018). Development of a new magnetic aluminum matrix nanocomposite. Ceram. Int. 44: 15079-15085.

Manikandan, R.; and Arjunan, T. (2020). Studies on micro structural characteristics, mechanical and tribological behaviours of boron carbide and cow dung ash reinforced aluminium (Al 7075) hybrid metal matrix composite. Compos. Part B Eng. 183: 107668.

Manimaran. R, Jayakumar. I, Mohammad; Giyahudeen, R. & Narayanan, L. (2018). Mechanical properties of fly ash composites—A review *Energy Sources, Part A: Recovery, Utilization and Environmental Effects* **40** 887–93.

Marcu, D. F.; Buzatu, M.; Ghica, V.G.; Petrescu, I. M.; and Popescu, G. (2018). Expermintal characterztation of aluminum based hybrid composites obtained through powder. In Proceedings of the IOP Conference Series Materials Science and Engineering; IOP Publishing: Tokyo, Japan. 374.

Mummoorthi, D.; Rajkumar, M.; and Kumar, S.G. (2019). Advancement and characterization of Al-Mg-Si alloy using reinforcing materials of Fe2O3 and B4C composite produced by stir casting method. J. Mech. Sci. Technol. 7: 3213–3222.

Narayan, S. & Rajeshkannan, A. (2011). Densification behaviour in forming of sintered iron-0.35% carbon powder metallurgy preform during cold upsetting *Materials & Design* **32,** 1006-13.

Negin, A., M.A. Azmah, Hanima, M. Sarraf., S. Sulaiman and Tang Sai Hong. (2020). Microstructural, Tribology and Corrosion Properties of Optimized Fe_3O_4 – SiC Reinforced Aluminium Matrix Hybrid Nano Fiber Composite Fabricated through Powder Metallurgy Method. 13: 4090.

Prakash, C.; Singh, S.; Sharma, S.; Garg, H.; Singh, J.; Kumar, and H.; Singh, G. (2020). Fabrication of aluminium carbon nano tube silicon carbide particles based hybrid Nano composite by spark plasma sintering. Mater. Today Proc. 21: 1637–1642.

Qiu, B; Xing, S; & Dong, Q. (2019). Fabrication and wear behavior of ZTA particles reinforced iron matrix composite produced by flow mixing and pressure compositing *Wear* 428–429 167–77.

Raghavan, V. (2009). Al-Fe-Si (aluminum-iron-silicon). *J. Phase Equilibrium Diffus.* 30: 184-188.

Ramakrishnan, A.; and Dinda, G. (2020). Microstructural control of an Al–W aluminum matrix composite during direct laser metal deposition. J. Alloy. Compd. 813: 152208.

Ravikumar, K.; Kiran, K.; and Sreebalaji, V. (2017). Characterization of mechanical properties of aluminium/tungsten carbide composites. Measurement. 102: 142–149.

Roshan, M. R., Mousavian, R. T., Ebrahimkhani, H., and Mosleh, A. (2013). Fabrication of Al-based Composites Reinforced with Al_2O_3-TiB_2 Ceramic Composite Particulates using Vortex-Casting Method. Journal of Mining and Metallurgy, Section B-Metallurgy, **49** (3): 299–305.

Sakthivelu, S. Sethusundaram, P. P. Ravichandran, M. and Meignanamoorthy, M. (2020). Experimental Investigation and Analysis of Properties and Dry Sliding Wear Behavior of Al -Fe-Si Alloy Matrix Composites. Silicon. doi:10. 1007/s12633-020-00662-4.

Salman, K.D.; Al-Maliki, W.A.K.; Alobaid, F.; and Epple, B. (2022). Microstructural Analysis and Mechanical Properties of a Hybrid Al/Fe2O3/Ag Nano-Composite. Appl. Sci. 12: 4730. https:// doi.org/10.3390/app12094730.

Samal, P; Vundavilli, P. R; Meher, A; & Mahapatra, M. M. (2020). Recent progress in aluminum metal matrix composites: A review on processing, mechanical and wear properties *Journal of Manufacturing Processes* **59** 131–52.

Saravanan, S. and Senthilkumar, M. (2015). "Mechanical Behavior of Aluminum (AlSi10Mg)-RHA Composite", International Journal of Engineering and Technology. 5(6): 4834-4840.

Sharma, S.; Nanda, T.; and Pandey, O. (2018). E ect of particle size on dry sliding wear behaviour of sillimanite reinforced aluminium matrix composites. Ceram. Int. 44: 104–114.

Sijo, M.; & Jayadevan, K. (2016). Analysis of stir cast aluminium silicon carbide metal matrix composite: A comprehensive review. Procedia Technol. 24, 379–385.
Singh, L; Singh; B; & Saxena, K. K. (2020). Manufacturing techniques for metal matrix composites (MMC): an overview *Advances in Materials and Processing Technologies* **6** 224–40.

Subri, N.W.B. M. Sarraf, B. Nasiri-Tabrizi, B. Ali, M.F. Mohd Sabri, W.J. Basirun, and N.L. Sukiman. (2020). Corrosion insight of iron and bismuth added Sn–1Ag–0.5 Cu lead-free solder alloy, Corrosion Engineering, Science and Technology. 55: 35-47.

Wang, L.; Yang, C.; Zhang, L.; Hu, Y.; Li, J.; Xu, S.; and Li, H.J.V. (2021). The exchange coupling interaction in CoFe2O4/Fe3O4 hard and soft magnetic nanocomposites. 181: 109751.

Wu, Z. X. D. H. Xiao., Z. M. Zhu., X. X. Li., and K. H. Chen. (2014). Effect of minor silver addition on microstructure and properties of Al-8Zn-1.Cu-1.3Mg-0.1Zr alloys. *Advanced Materials Research*. 834-836 (31): 360-363.